6.3 The Impact of Simulated GEMS Observations on Regional Weather Forecasts

Joseph G. Dreher*, John Manobianco, and Mark L. Adams
ENSCO, Inc., Melbourne, FL

1. INTRODUCTION

Technological advancements in Micro Electro Mechanical Systems (MEMS) and nanotechnology have inspired a concept for a revolutionary observing system called Global Environmental Micro Sensors (GEMS). The system features a wireless network of in situ, buoyant airborne probes that can monitor all regions of the Earth with unprecedented spatial and temporal resolution. The probes will be designed to remain suspended in the atmosphere for hours to days and take measurements of temperature, humidity, pressure, and wind velocity that are commonly used as dependent variables in numerical weather prediction (NWP) models. As a result, it will not be necessary to develop complex algorithms for assimilating such data into research or operational models.

This paper provides a discussion of the system used to simulate dispersion of and observations collected by an ensemble of probes, highlights a possible deployment scenario and describes a series of Observing System Simulation Experiments (OSSEs) performed to assess the impacts of simulated GEMS data on regional weather forecasts.

2. SIMULATION SYSTEM

The Advanced Regional Prediction System (ARPS; Xue et al. 2000; Xue et al. 2001) coupled with a Lagrangian particle model (LPM) is used to simulate the dispersion of observations collected by an ensemble of probes. The ARPS is a complete, fully automated, stand-alone system designed to forecast explicitly storm- and regional-scale weather phenomena. It includes a data ingest, quality control, and objective analysis package known as ADAS (ARPS Data Analysis System; Brewster 1996), a prediction model, and a post-processing package.

Probe dispersion is simulated using the LPM embedded within ARPS. The probes are assumed to be passive tracers moving independent of one another and transported by the wind. The LPM tracks the location of each probe based on three-dimensional wind components and updates probe position using the resolvable-scale components of wind velocity directly from the ARPS model, as well as turbulent velocity fluctuations. The turbulent velocity fluctuations are estimated from a subgrid scale (SGS) turbulence parameterization (Mellor and Yamada 1980) similar to the SGS turbulence scheme of Deardorff (1980) used in the ARPS model. A parameterization scheme for wet deposition or precipitation scavenging is included in the LPM to simulate the impact of frozen and liquid precipitation on probe trajectory and possible washout (Seinfield and Pandis 1998). Scavenging was designed to cause probes to alter trajectories and washout, especially in areas of heavy rain near the surface.

*Corresponding author address: Joseph G. Dreher, ENSCO, Inc., 4849 N. Wickham Rd., Melbourne, FL 32940. e-mail: dreher.joe@ensco.com

3. DEPLOYMENT SCENARIO

A large number ($>10^6$) of simulated probes can be deployed at any time during the model integration, and at any latitude, longitude, and altitude within the three-dimensional ARPS domain. The LPM provides accurate position information because the velocity variables are updated every model time step by interpolating to the actual probe locations.

Two 30-day periods from June and December 2001 were selected to study the dispersion characteristics of GEMS under differing weather regimes. The summer case was chosen to assess probe dispersion during a weather pattern with relatively weak large-scale flow, and the winter case was selected to analyze probe dispersion with strong jet streams and progressive large-scale features. The differences in simulated probe dispersion were expected to be substantial depending on the prevailing weather patterns, so it was important to study the dispersion patterns under two widely varying weather scenarios.

A strategy to deploy positively buoyant probes that ascend upward through the atmosphere was developed. For this scenario, simulated probes were released from surface weather station sites around the northern hemisphere and ascended to a level of neutral buoyancy that depends on probe mass. This scenario examines the impact of probes remaining neutrally buoyant throughout 30-day simulations versus becoming negatively buoyant and falling out of the air gradually. Depictions of the resulting probe distribution for both June and December 2001, over the northern hemisphere after 14 days are shown in Figure 1.

4. REGIONAL OSSEs

OSSEs are used to assess the impact of probe measurements on weather analyses and forecasts following Atlas (1997) and Lord (1997). The model used for OSSEs is the Pennsylvania State University

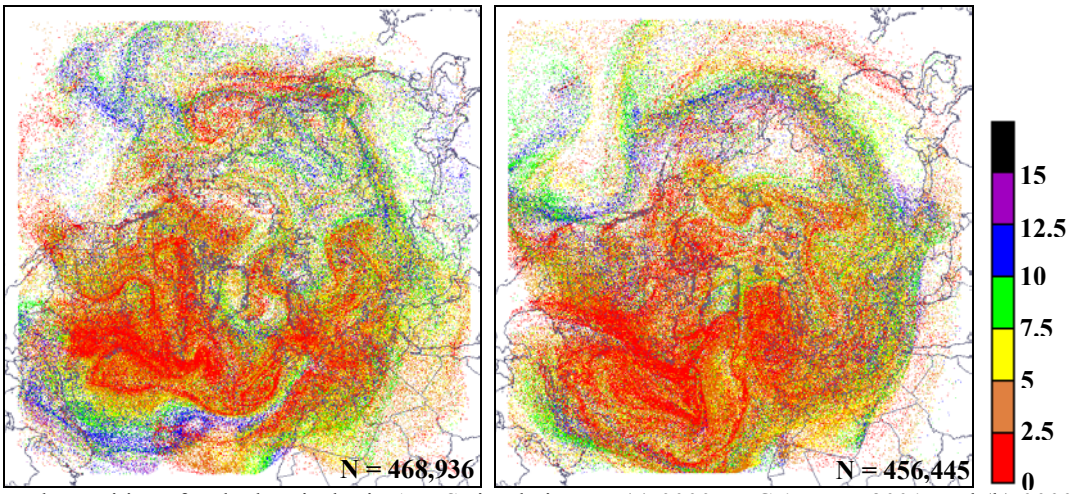

Figure 1. Probe positions for the hemispheric ARPS simulations at (a) 0000 UTC 15 June 2001, and (b) 0000 UTC 15 December 2001, 14 days after model initialization time. The probe altitude (km) is denoted by the colors according to the key provided and total number of probes is given by N.

(PSU)/National Center for Atmospheric Research (NCAR) Fifth-generation Mesoscale Model (MM5; Grell et al. 1995). The MM5 is configured in such a manner as to generate a significantly different solution from a nature simulation to approximate the differences between a state-of-the-art model and the real atmosphere (Atlas 1997). For this study, two 30-day periods during June and December 2001 . The OSSE methodology consists of three steps:

- **Nature simulations.** These forecast runs are considered "truth" and the trajectories of all simulated probes are tracked and extracted. In addition to simulated GEMS data all surface, rawinsonde and aircraft data are extracted from these model simulations as well. The ARPS model is used for the nature simulations.

- **Conventional simulations (Cnv)**. Simulated surface, rawinsonde, and aircraft observations are intermittently assimilated into the MM5 at specified times.

- **Conventional & GEMS simulations (CnvGEMS)**. In addition to conventional data, simulated GEMS data are intermittently assimilated into the MM5 at specified times.

4.1 Nature Runs

Two ARPS 50-km hemispheric nature runs (domain A, Figure 2) were initialized using Aviation Model (AVN) re-analysis fields (1° x 1°) from 0000 UTC 1 June 2001 and 0000 UTC 1 December 2001, respectively, and run for 30 days to simulate large-scale dispersion of GEMS probes. The AVN grids were also used to provide lateral boundary conditions at 12-h intervals throughout each model run (Kalnay et al. 1996). A one-way nested 15-km domain covering a large portion of the United States and Canada (domain B, Figure 2) was initialized at 0000 UTC 10 June 2001 and 0000 UTC 10 December 2001, respectively, and run 10 days. For each 15-km ARPS simulation, lateral boundary conditions were supplied by the ARPS 50-km simulation at 3-h intervals. Simulated measurements from conventional networks and GEMS probes were extracted at 3-h intervals during each 15-km ARPS simulation.

To simulate measurements obtained from probes and conventional observational networks, interpolation was used to extract values of temperature, humidity, pressure, cloud water, and other model variables at locations throughout the nature model integration. By assuming the probes are passive tracers, temporal changes in their absolute or relative position were used to estimate wind velocities. Additionally, a random component to represent observation error was added to address questions of instrument accuracy.

4.2 Regional Assimilation Runs

MM5 60-km hemispheric runs were initialized at 0000 UTC 10 June and 0000 UTC 10 December 2001 using the ARPS 50-km nature simulations. The MM5 grid covers approximately the same area as domain A in Figure 2. AVN re-analysis fields supplied lateral boundary conditions at 12-h intervals throughout each model run.

The MM5 30-km simulations, covering approximately domain B in Figure 2, were initialized at 0000 UTC 11 June and 0000 UTC 11 December 2001, respectively, in a one-way nested configuration from the MM5-60-km simulations and run until 0000 UTC 18 June and 0000 UTC 18 December 2001,

respectively. Simulated conventional and/or GEMS data obtained from the ARPS 15-km simulations were intermittently assimilated into the MM5 at 3-h intervals throughout each run. For both 30-km MM5 experiments, the 60-km MM5 simulations supplied the lateral boundary conditions. An illustration of both the ARPS nature and MM5 OSSE methodology is shown in Figure 3.

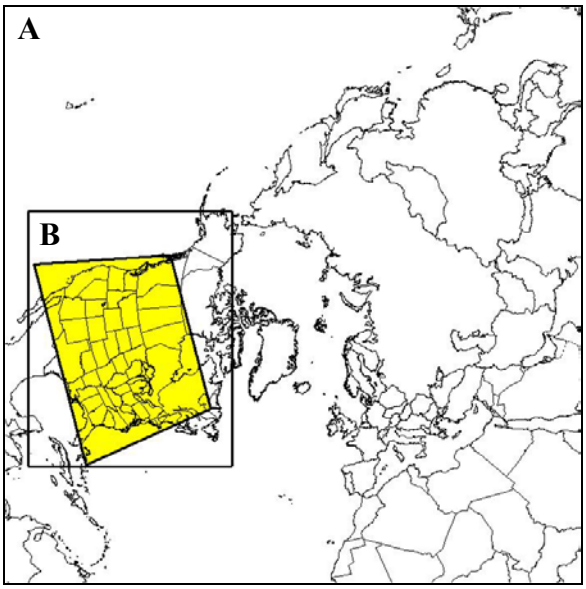

Figure 2. Grid configuration for the ARPS nature and MM5 OSSE simulations. Grid A represents the outer ARPS 50-km and MM5 60-km domains, while grid B denotes the ARPS 15-km and MM5 30-km domains, respectively. Yellow-shaded box represents area of objective verification statistics described in section 5.

Data were assimilated into the MM5 using an intermittent data assimilation (DA) technique similar to Rogers et al. (1996) and Manobianco (2002) and depicted in This technique incorporated simulated data from the ARPS model runs into the MM5 integration by using a two successive-scan Cressman scheme with quality-control checks that subsequently adjusts the analyses from the first guess towards the observations at 3-h intervals. Each 3-h background field contains information from the previous observations through the analysis and forecasts of MM5. This cycle was repeated every 3-h throughout the seven day forecast periods for both June and December 2001.

Since the regional lateral boundary conditions tend to propagate through the regional simulations, especially at later forecast times (Warner et al. 1997), the domains were chosen as large as computationally practical. Furthermore, simulated conventional data (rawinsonde, surface, and aircraft) were assimilated into each MM5 60-km run at 12-h intervals to provide better initial and boundary conditions.

In order to mimic a regional operational forecast cycle, 48-h forecasts were generated at 6-h intervals during the intermittent DA cycle for both the June and December 2001 OSSEs following Weygandt et al. 2004. A total of 29 forecasts were conducted for each OSSE scenario. A summary of the dates and duration of the regional OSSE forecasts is presented in Table 1.

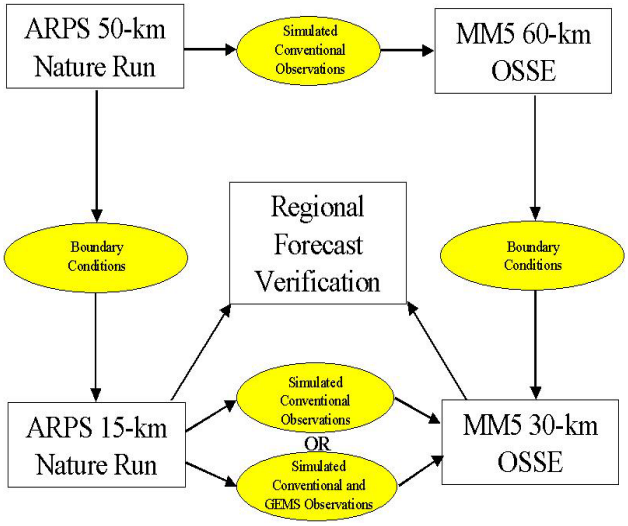

Figure 3. Flowchart for the nature run and OSSEs. Boundary conditions for the ARPS 50-km and MM5 60-km simulations were supplied by AVN re-analysis fields.

4.3 Conventional OSSEs (Cnv)

The Cnv OSSEs include only in situ data from simulated conventional networks. The Cnv simulations serve as a point of reference against which the experiments are compared, since no simulated GEMS observations were included.

4.4 Conventional & GEMS (CnvGEMS)

In addition to simulated conventional data the CnvGEMS OSSEs includes simulated data obtained from the GEMS surface deployment scenario. All simulated data (conventional and GEMS) were assimilated into the MM5 30-km OSSEs at 3-h intervals.

5. REGIONAL OSSE VERIFICATION

In order to verify the realism of the OSSEs (defined by Hamill and Colucci 1997), the nature runs were interpolated to a grid identical to that of the MM5 30-km simulations. Objective verification of the OSSEs was then accomplished by calculating gridded root mean square (RMS) errors over a sub-domain centered on much of the United States.

Table 1. Summary of the regional OSSE forecasts for both the June and December 2001 experiments.

Simulation	Dates	Duration	Experiment
Regional nature run – ARPS 15-km simulations	10-20 June and December	10 days	ARPS regional forecast
	10-11 June and December	1 day	ARPS 15-km spin-up
	11-18 June and December	7 days	Simulated observations extracted at 3-h intervals (simulated rawinsonde extracted at 12-h intervals)
Regional OSSEs – MM5 30-km simulations	11-18 June and December	7 days	Intermittent DA cycle with 3-h update cycle using ARPS simulated observations
	11-18 June and December	7 days	Generation of 48-h forecasts at 6-intervals
	11-20 June and December	9 days	Verification of MM5 forecasts against ARPS nature simulations

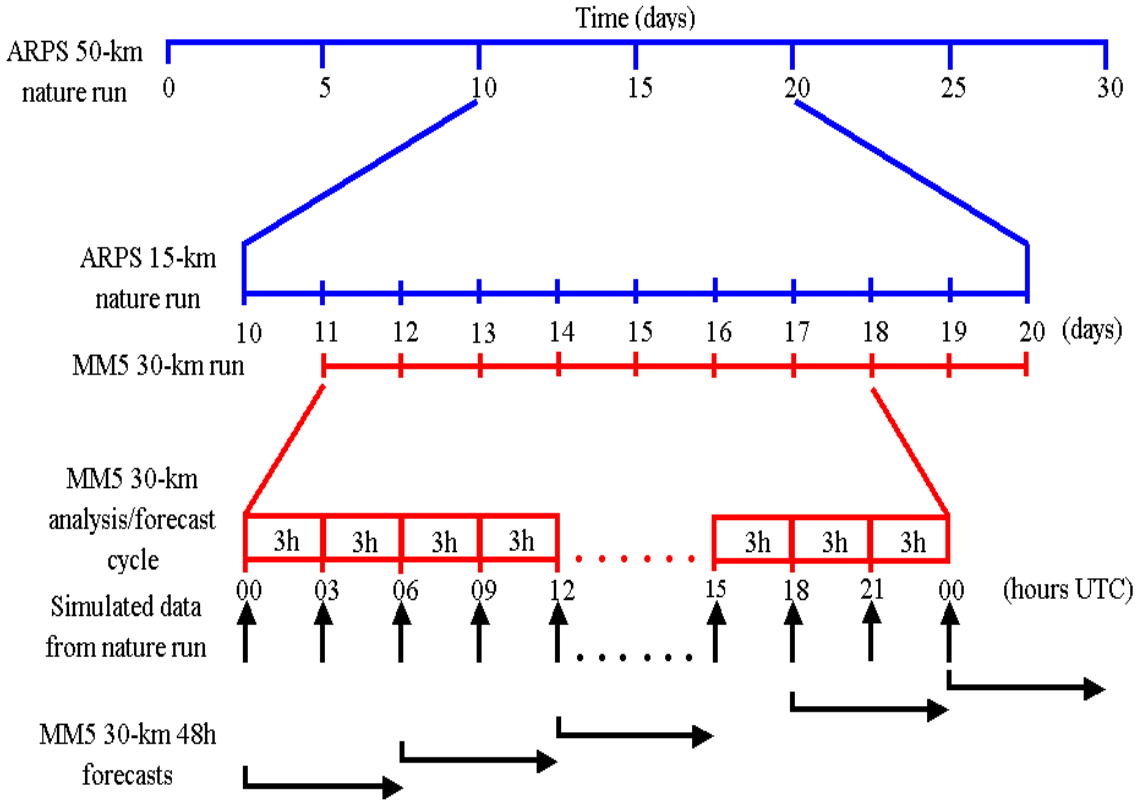

Figure 4. Schematic of the regional OSSEs timeline and data assimilation methodology.

If Φ represents a predicted variable from the OSSEs, then forecast error is defined as:

$$\Phi' = \Phi_{exp} - \Phi_{nat}, \quad (1)$$

where the subscripts *exp* and *nat* denote the experiment (OSSE) and nature quantities, respectively. The RMS error is calculated as:

$$\text{RMS Error} = \sqrt{\frac{1}{N}\sum_{i=1}^{N}(\Phi')^2}, \quad (2)$$

where N represents the total number of grid points (171 X 203) times the number of forecasts (29) at any given height in the atmosphere. Furthermore, the forecast impact was normalized by computing an improvement relative to the control (Cnv) forecasts as follows:

$$\%\ \text{Improvement} = 100 \times \frac{\text{CNTL - EXP}}{\text{CNTL}}, \quad (3)$$

where CNTL are the Cnv RMS errors and EXP (CnvGEMS) are the experiment errors. Positive (negative) values indicate improved (worsened) impact of the assimilated data on the forecasts.

A total of 9 sensitivity OSSEs were conducted and the details of each experiment are summarized in Table 2 along with the ARPS nature simulations. Each OSSE, with the exception of Experiment 5, assumed perfect observations with no instrument errors. In Experiment 5, random errors for the simulated probes were added to each variable, based on typical errors for MEMS sensors (Kristofer S. J. Pister, personal communication). In addition, random errors were added to each variable for the simulated conventional observations. A description of the random errors consistent with each observation is given in Table 3, along with approximate observation data counts for 0000 UTC and 0300 UTC. The results of these OSSEs are presented in the next section and compared to the ARPS nature simulations.

Experiments 8 and 9 reduced the total number of probes by 90% and 99%, respectively. Data thinning was performed by excluding probes randomly, without replacement, throughout the assimilation domain to reduce the effective resolution of the assimilated data. Once a probe was randomly excluded, the probe was removed from all subsequent data assimilation times, similar to releasing probes less often from the surface deployment scenario. To verify the realism of randomly thinning data, the deployment scenario was modified to release probes less often, effectively reducing the number of probes at later times. Overall, randomly thinning without replacement and changing the deployment scenario were found to give very similar forecast results.

6. REGIONAL OSSE RESULTS

Overall, both the June and December 2001 OSSEs demonstrated the assimilation of simulated GEMS observations improves the predicted primary variables compared with assimilating only conventional data.

To diagnose the distribution of impacts throughout the entire troposphere, vertical profiles of RMS errors as a function of forecast hour (0-h, 12-h and 24-h) were plotted (Figure 5 and Figure 6). Additionally, vertical profiles of percent improvement of the RMS forecast errors were generated for both the June and December OSSE scenarios (Figure 7 and Figure 8). The percent improvement profiles were further stratified by forecast initialization times with (0000 and 1200 UTC) and without (0600 and 1800 UTC) the availability of standard rawinsonde data. The impact of GEMS data was expected to be greater at the non-rawinsonde initialization times when there is substantially less conventional in situ data above the surface.

Experiment 1 – Cnv

Exp. 1 included simulated conventional observations and all sampled meteorological variables were assimilated into both the June and December 2001 OSSEs. These experiments were designed to emulate an operational regional forecast assimilation system and serve as a point of reference to benchmark the other experiments.

Experiment 2 – CnvGEMS

Exp. 2 included both simulated conventional and GEMS data from both the June and December OSSEs.

6.1 June 2001

The vertical profiles of RMS errors for the June 2001 experiments indicate large error reductions for each variable as benchmarked against Experiment 1 (Figure 5). The largest RMS error differences occur for the 0-h forecasts when GEMS data have most impact on the analysis creating better initial conditions. However, those effects are diminished at later times (12-h and 24-h) due to the influence of the lateral boundary conditions. It is important to note, that the smaller RMS error differences below 900-hPa for each variable are likely due to the impact of the conventional surface data. In this case, there are few near-surface GEMS observations and they are competing against conventional data

The vertical distribution of the percent improvement profiles generally demonstrates a larger improvement for the non-rawinsonde initialization times when simulated GEMS observations are competing with less conventional observations. Overall, the CnvGEMS 0-h forecasts showed

Table 2. Summary of the simulations and regional OSSE experiments for June 2001 and December 2001. For each experiment, the variables assimilated into the OSSE (if applicable) are provided, along with a description of experiment. Experiment descriptions are only given for the regional ARPS 15-km and MM5 30-km simulations, respectively. Sensitivity experiments 3-8 were conducted only for June 2001.

Simulations	Variables Assimilated	Experiment Description
Nature	N/A	ARPS 30-day run.
OSSE Experiment 1 (June and December 2001)	T, p, T_d, u, v*	Simulated surface, rawinsonde, and aircraft observations assimilated into MM5.
OSSE Experiment 2 (June and December 2001)	T, p, T_d, u, v	Same as Exp. # 1, except that in addition to conventional data, simulated GEMS data are assimilated into MM5
OSSE Experiment 3 (June 2001)	T, p, u, v	Same as Exp. #2, but exclude T_d
OSSE Experiment 4 (June 2001)	T, p, T_d	Same as Exp. #2, but exclude u, v (winds)
OSSE Experiment 5 (June 2001)	T, p, T_d, u, v	Same as Exp. #2, but include random probe and conventional observation errors
OSSE Experiment 6 (June 2001)	T, p, T_d, u, v	Same as Exp. #2, but include precipitation scavenging of probes
OSSE Experiment 7 (June 2001)	T, p, T_d, u, v	Same as Exp. #2, but use a 6-h intermittent data assimilation cycle
OSSE Experiment 8 (June 2001)	T, p, T_d, u, v	Same as Exp. #2, but use only 10% of GEMS data
OSSE Experiment 9 (June 2001)	T, p, T_d, u, v	Same as Exp. #2, but use only 1% of GEMS data
*T = temperature, p = pressure, T_d = Dewpoint, u = u-wind component, v = v-wind component.		

Table 3. Observations simulated from the ARPS regional nature runs. The variables and assigned errors used in experiment 5 are given for each observation type. Approximate observation counts for 0000 UTC and 0300 UTC June and December 2001 are also shown.

Observation Type	Variables	Random Error (Exp. 5)	Number of Observations	
			0000 UTC	0300 UTC
Rawinsonde	Temperature Dew point Pressure u- / v- winds	± 0.5 K ± 2 K ± 1 hPa ± 1 m s^{-1}	219	0
Aircraft	Temperature Pressure u- / v- winds	± 0.5 K ± 1 hPa ± 1.1 m s^{-1}	1,553	2,140
Surface	Temperature Dew point Pressure u- / v- winds	± 0.5 K ± 1 K ± 1 hPa ± 1 m s^{-1}	2,337	2,337
GEMS	Temperature Dew point Pressure u- / v- winds	± 0.5 K ± 2 K ± 1 hPa ± 1 m s^{-1}	115,881 – 11 June 92,904 – 11 Dec	115,620 – 11 June 92,792 – 11 Dec

improvements >30% for each variable and throughout the depth of the troposphere (Figure 7). The percent improvements for the 12-h and 24-h forecasts were smaller; however even for the 24-h forecasts of dewpoint, the improvement reaches a maximum of 35% above 250-hPa (Figure 7f).

6.2 December 2001

Overall the results from the December 2001 OSSE were very similar to the results from June 2001. The vertical profiles of RMS errors show large error differences throughout the troposphere, especially at the 0-h and 12-h forecasts, between Exps. 1 and 2 (Figure 6). However, there were smaller vector wind error differences than June 2001, for the 24-h forecasts due to the influence of lateral boundary conditions (Figure 6). This is consistent with point made by Warner et al. 1997 that the lateral boundary impacts would be larger for a stronger flow regime (December) than for a weaker flow regime (June).

As expected the largest percent improvement occurred for non-rawinsonde initialization times. Notable in the dewpoint percent improvement statistics is the larger forecast impact (75% at 0-h, 50% at 12-h and 40% at 24-h) above the 250-hPa level (Figure 8). The large percent improvements are likely due to the fact that the simulated conventional aircraft data suite does not include moisture data.

The slight negative improvements, or forecast degradation, above 200 hPa at 12-h and 24-h is likely due to the lateral boundary condition errors that have reached the verification domain (Figure 8b,h,c,i). No such forecast degradations were evident in the June OSSEs.

6.3 Sensitivity Analysis

For brevity, the results for June 2001 sensitivity experiments are summarized without accompanying figures in the sections that follow:

Experiment 3 – No Dewpoint

Exp. 3 included the same GEMS data as Exp. 2 but the dewpoint variable was excluded from the DA cycle. The most significant impact of excluding dewpoint data was that dewpoint RMS errors were very similar to Exp. 1 dewpoint errors at all forecast times and levels. There was a slight increase in the vector wind RMS errors at all forecast times and throughout the troposphere. Excluding dewpoint data had no significant impact on the temperature RMS errors.

Experiment 4 – No Wind

Exp. 4 included the same GEMS data as in Exp. 2 but both the u and v components of the wind were withheld from the DA cycle. By excluding wind data, the magnitude of the vector wind errors degraded to that of the Exp. 1. Interestingly, by excluding wind data both the temperature and dewpoint RMS errors increased below 250-hPa, especially for the 12-h and 24-forecasts. In fact, the temperature and dewpoint RMS errors at 24-h approach the magnitudes of the RMS errors from Exp. 1 at 24-h.

Experiment 5 – Instrument Errors

Exp. 5 included the same GEMS and conventional data as Exp. 2, but with random observational errors. Introducing errors caused little degradation in the temperature, dewpoint and vector wind forecasts when compared with Exp. 2.

Experiment 6 – Precipitation Scavenging

For Exp. 6 the simulated GEMS data were extracted from an ARPS nature simulation where probe precipitation and ice scavenging was activated in the LPM. Precipitation scavenging made very little difference in the temperature and dewpoint errors, except for slight degradation of the temperature RMS errors below 400-hPa (especially for the 24-h forecasts by approximately 0.25 K). The largest differences were in the vector wind RMS errors with degradation at all levels and forecast times when precipitation scavenging was activated. Vector wind RMS errors were approximately 0.25 ms^{-1} higher at all levels for the 0-h and 12-h forecasts when comparing the RMS errors to Exp. 2. However, for the 24-h forecasts, the Exp. 5 RMS errors approach the magnitude of those from Exp.1 at 24-h

Experiment 7 – 6-h DA Frequency

Exp. 7 included the same probes and conventional data as in Exp. 2, but all simulated data were assimilated at 6-h instead of 3-h intervals. This experiment was designed to test the sensitivity of data assimilation frequency. By assimilating the data less often at 6-h intervals, the RMS errors for all variables do not show degradation when compared to Exp. 2.

Experiment 8 - 10% of probe data

Excluding 90% of the probes from the DA cycle did not substantially degrade the 48-h forecasts of temperature, dewpoint and vector wind when comparing the RMS errors to the full data set used for Exp. 2.

Experiment 9 – 1% of probe data

Excluding 99% of the probes from the DA cycle and subsequent 48-h forecasts substantially degraded the forecasts of temperature, dewpoint and vector wind when comparing the RMS errors to the full data set used for Exp. 2. For all variables and forecast times the

errors approach the magnitudes of Exp. 1 errors, especially for the 12-h and 24-h forecasts. Excluding 99% of the GEMS data provided relatively little forecast improvement over the Cnv simulation.

7. SUMMARY AND CONCLUSIONS

A series of regional OSSEs has been completed during two different weather regimes to evaluate the potential impact on forecasts from a proposed in situ measurement system known as GEMS. Experiments were designed to evaluate the added benefit of GEMS to a conventional data network. The OSSEs demonstrated that the addition of simulated GEMS observations extracted from the nature simulation had a significant impact on improving the predicted primary variables over the conventional simulations. The results indicate that the improvements to the regional forecast skill exceed 50%, especially for the 0-h forecasts. The forecasts impacts were generally similar for both the June and December OSSEs. The only notable exception was that the impacts of the simulated GEMS data are lost sooner for the December 2001 OSSEs due to inward prorogation of the lateral boundary conditions.

Most importantly, sensitivity experiments indicated that the OSSEs produced a positive impact on the forecasts with a significantly reduced (90%) number of probes. Additionally, the OSSEs produced nearly identical results from assimilating data at 6-h intervals instead of 3-h intervals. However, activating precipitation scavenging in the nature simulations did have an impact on the subsequent forecasts. The degradation was most apparent in the vector wind forecasts at later forecast times (24-h); but the improvement was still substantially greater than the conventional simulations. The data denial experiments indicated that the maximum forecast impacts were realized when the simulated GEMS data provided a full suite of measurements. Finally, the inclusion of random errors in both the simulated GEMS and conventional data did not substantially degrade the forecasts.

Based on the results obtained from these regional OSSEs, further work dealing with GEMS simulated probes is planned. Experiments are currently underway to validate the OSSEs by comparing the forecast impact to assimilating real observations (following Weygandt et al. 2004).

8. ACKNOWLEDGEMENTS

This work was supported by the Universities Space Research Association's NASA Institute for Advanced Concepts.

9. REFERENCES

Atlas, R., 1997: Atmospheric observations and experiments to assess their usefulness in data assimilation. *J. Royal Meteor. Soc. Japan*, **75**, 111-130.

Brewster, K., 1996: Application of a Bratseth analysis scheme including Doppler radar data. Preprints, *15th Conf. on Weather Analysis and Forecasting*, Amer. Meteor. Soc., Norfolk, VA, 92-95.

Deardorff, J. W., 1980: Stratocumulus-capped mixed layers derived from a three-dimensional model. *Bound.-Layer Meteor*., **7**, 199-226.

Grell, G., J. Dudhia, and D. Satuffer, 1995: A description of the Fifth-Generation Penn State/NCAR mesoscale model (MM5). NCAR / TN-398 + STR [Available on line at http://www .mmm.ucar.edu/mm5/mm5-home.html].

Hamill, T., M., and S., J., Colucci, 1997: Verification of Eta–RSM Short-Range Ensemble Forecasts. *Mon. Wea. Review*, **125**, 1312–1327.

Kalnay, E., and Coauthors, 1996: The NCEP/NCAR 40-year reanalysis project. *Bull. Amer. Meteor. Soc*., **77**, 437-471.

Lord, S. J., E. Kalnay, R. Daley, G. D. Emmitt, and R. Atlas, 1997: Using OSSEs in the design of the future generation of integrated observing systems. Preprints, *First Symposium on Integrated Observing Systems*, Amer. Meteor. Soc., Long Beach, CA, 45-47.

Manobianco, J., 2002: Global Environmental MEMS Sensors (GEMS): A Revolutionary Observing System for the 21st Century, Phase I Final Report. [Available online at http://www.niac. usra.edu/studies/].

Mellor, G. L., and T. Yamada, 1982: Development of a turbulence closure model for geophysical fluid problems. *Rev. Geophys. Space Phys*., **20**, 851-875.

Nutter, P. A., and J. Manobianco, 1999: Evaluation of the 29-km Eta model. Part I: Objective verification at three selected stations. *Wea. Forecasting*, **14,** 5-17.

Rogers, E., T. L. Black, D. G. Deaven, G. J. DiMego, Q. Zhao, M. Baldwin, N. W. Junker, and Y. Lin, 1996: Changes to the operational "early" eta analysis/forecast system at the National Centers for Environmental Prediction. *Wea. Forecasting,* **11,** 391-413.

Seinfeld, J. H., and S. N. Pandis, 1998: *Atmospheric Chemistry and Physics – From Air Pollution to Climate Change*, John Wiley and Sons Inc., New York, 1326 pp.

Warner, T.T., Peterson, R.A. and Treadon, R.E. (1997): A tutorial on lateral boundary conditions as a basic and potentially serious limitation to regional numerical weather prediction. *Bull. Amer. Meteor. Soc*., **78**, 2599–2617.

Weygandt, S.S., and coauthors, 2004: Potential forecast impacts from space-based lidar winds: Regional observing system simulation experiments. *8thSymp. Int. Obs. and Assim. Systems for Atm. Oceans and Land Surf.,* Seattle, Amer. Meteor. Soc.

Xue, M., K. K. Droegemeier, and V. Wong, 2000: The Advanced Regional Prediction System (ARPS) — A multi-scale nonhydrostatic atmospheric simulation and prediction model. Part I: Model dynamics and verification. *Meteor. Atmos. Phys.*, **75**, 161-193.

_____, and Coauthors, 2001: The Advanced Regional Prediction System (ARPS) — A multiscale nonhydrostatic atmospheric simulation and prediction tool. Part II: Model physics and applications. *Meteor. Atmos. Phys*., **76**, 143-165.

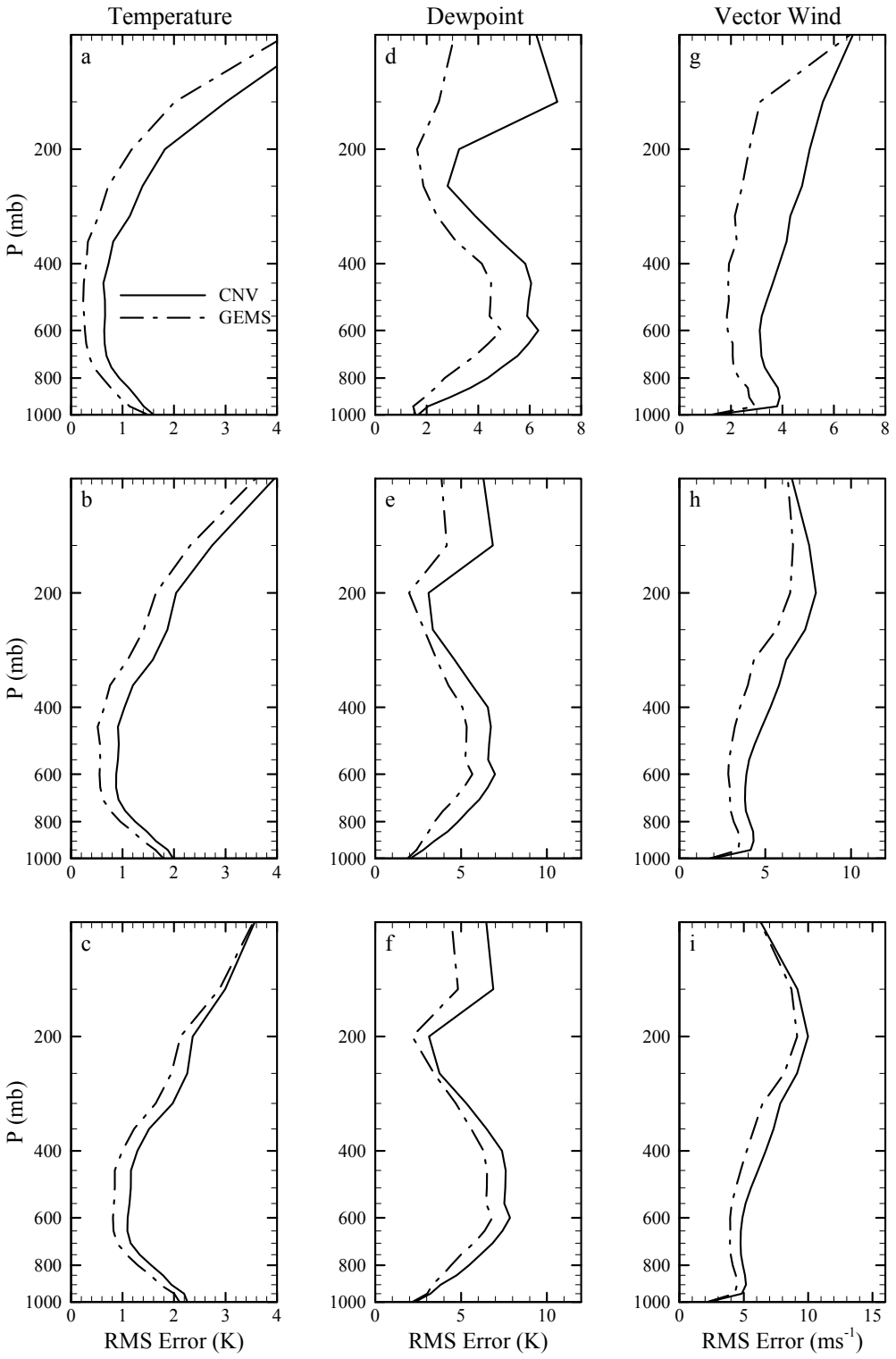

Figure 5. Vertical profiles of the temperature (a-c), dew point (d-f), and vector wind (g-i) root mean square (RMS) error for the conventional and GEMS OSSE forecasts from June 2001. Data are presented for the 0-h (a,d,g), 12-h (b,e,h), and 24-h (c,f,i) forecasts. Statistics were computed over the OSSE verification domain shown in Figure 2.

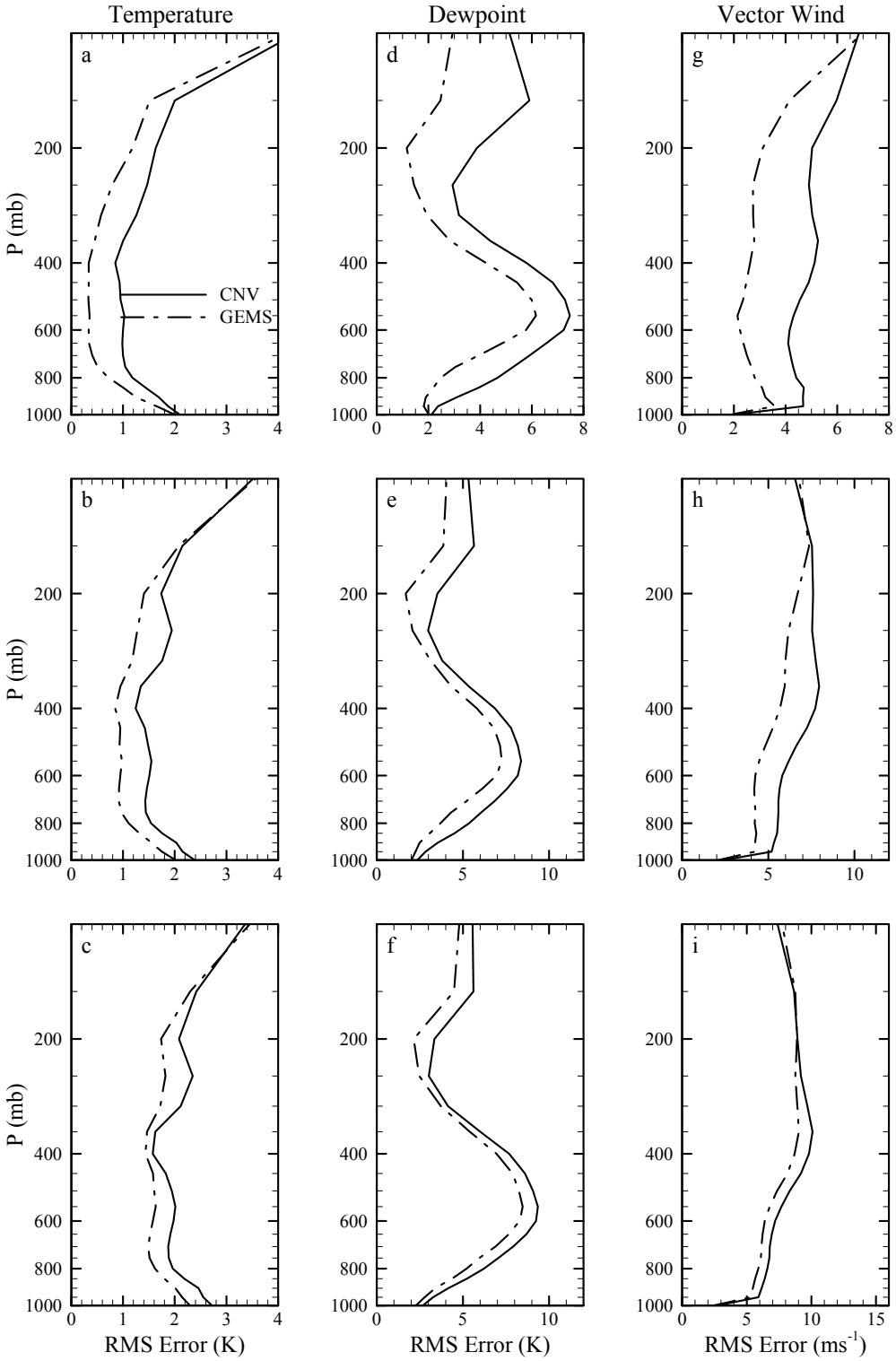

Figure 6. Vertical profiles of the temperature (a-c), dew point (d-f), and vector wind (g-i) root mean square (RMS) error for the conventional and GEMS OSSE forecasts from December 2001. Data are presented for the 0-h (a,d,g), 12-h (b,e,h), and 24-h (c,f,i) forecasts. Statistics were computed over the OSSE verification domain shown in Figure 2.

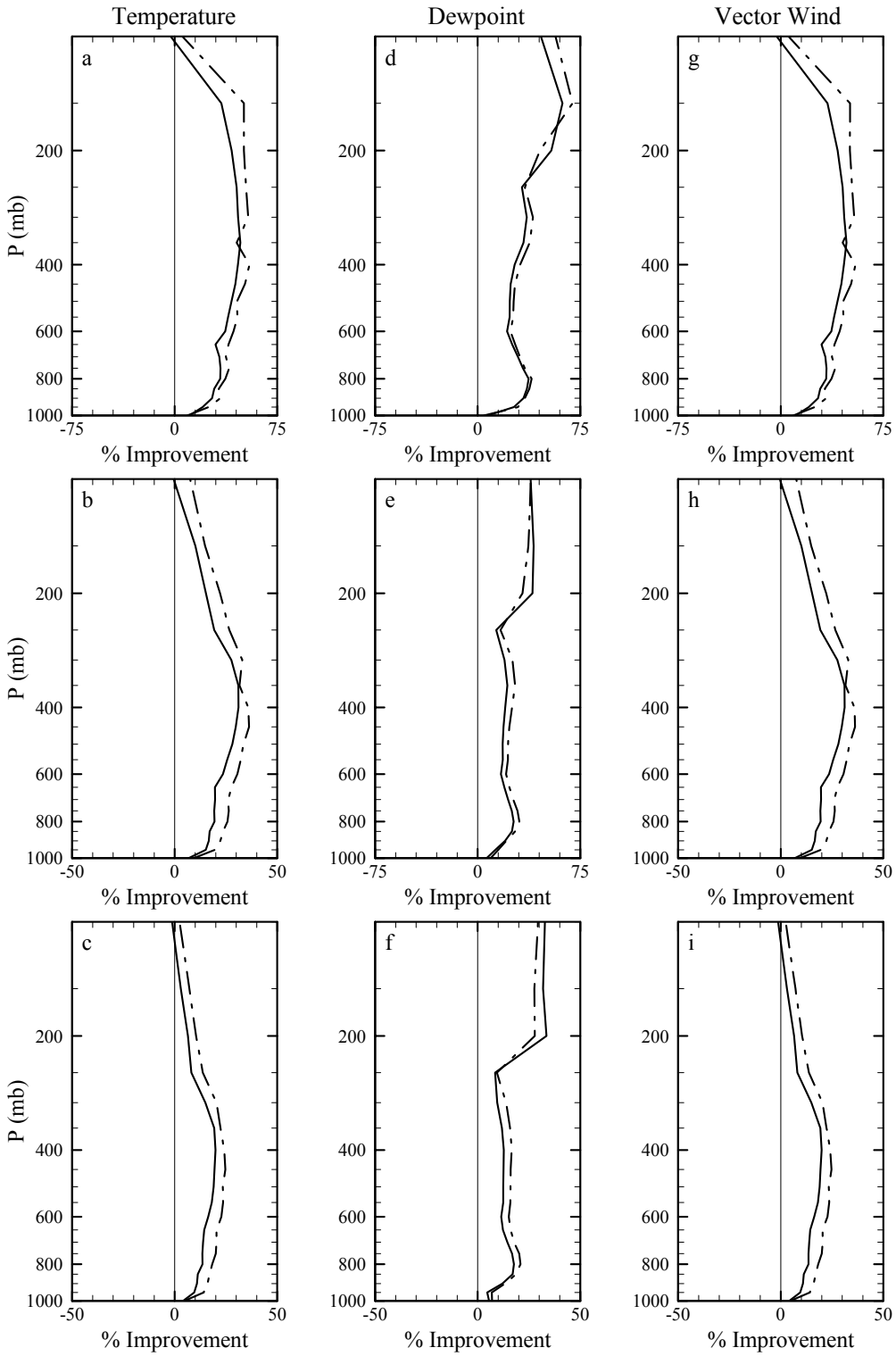

Figure 7. Vertical profiles of the temperature (a-c), dew point (d-f), and vector wind (g-i) percent improvement for the GEMS OSSE forecasts from June 2001 shown for rawinsonde (solid line) and non-rawinsonde initialization (dashed line) times. Data are presented for the 0-h (a,d,g), 12-h (b,e,h), and 24-h (c,f,i) forecasts. Statistics were computed over the OSSE verification domain shown in Figure 2.

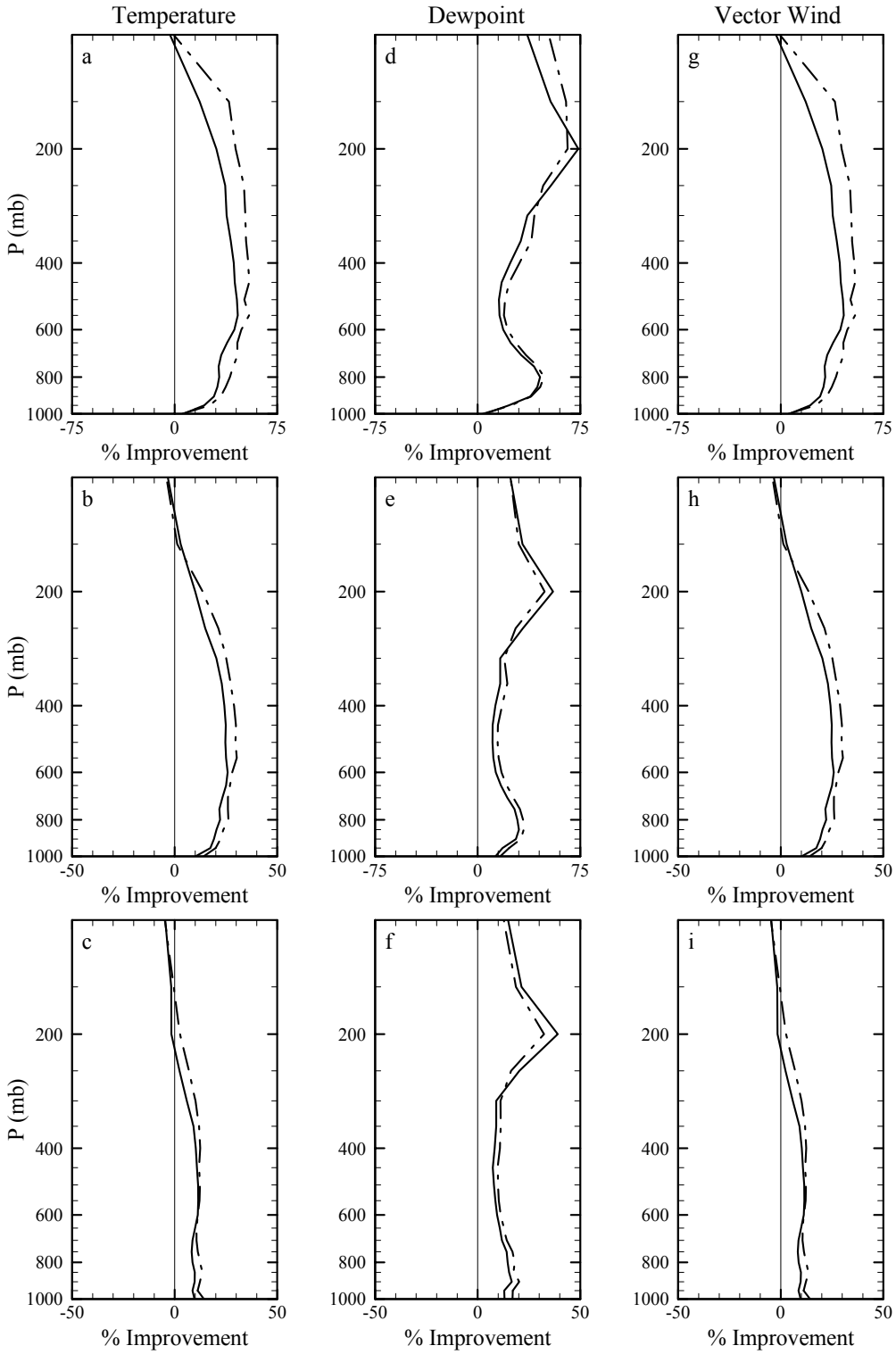

Figure 8. Vertical profiles of the temperature (a-c), dew point (d-f), and vector wind (g-i) percent improvement for the GEMS OSSE forecasts from December 2001 shown for rawinsonde (solid line) and non-rawinsonde initialization (dashed line) times. Data are presented for the 0-h (a,d,g), 12-h (b,e,h), and 24-h (c,f,i) forecasts. Statistics were computed over the OSSE verification domain shown in Figure 2.